Coupling of a single-photon emitter in nanodiamond to surface plasmons of a nanochannel-enclosed silver nanowire

Morteza Aramesh,[1,2] Jiri Cervenka,[1] Ann Roberts,[1] Amir Djalalian-Assl,[1] Ranjith Rajasekharan,[1] Jinghua Fang,[2] Kostya Ostrikov,[2] and Steven Prawer[1,*]

[1]*Physics Department, the University of Melbourne, Melbourne, 3010, VIC, Australia*
[2]*The Commonwealth Scientific and Industrial Research Organisation (CSIRO), Plasma Science and Technology, Lindfield, Sydney, 2070, NSW, Australia*
[*]*s.prawer@unimelb.edu.au*

Abstract: A finite element method is applied to study the coupling between a nitrogen vacancy (NV) single photon emitter in nanodiamond and surface plasmons in a silver nanowire embedded in an alumina nanochannel template. We investigate the effective parameters in the coupled system and present detailed optimization for the maximum transmitted power at a selected optical frequency (650 nm). The studied parameters include nanowire length, nanowire diameter, distance between the dipole and the nanowire, orientation of the emitter and refractive index of the surrounding. It is found that the diameter of the nanowire has a strong influence on the propagation of the surface plasmon polaritons and emission power from the bottom and top endings of the nanowire.

OCIS codes: (240.6680) Surface plasmons; (230.7370) Waveguides; (230.0230) Optical devices.

References and links

1. J. Yang, G. W. Lin, Y. P. Niu, and S. Q. Gong, "Quantum entangling gates using the strong coupling between two optical emitters and nanowire surface plasmons," Opt. Express **21**(13), 15618–15626 (2013).
2. K. J. Savage, M. M. Hawkeye, R. Esteban, A. G. Borisov, J. Aizpurua, and J. J. Baumberg, "Revealing the quantum regime in tunnelling plasmonics," Nature **491**(7425), 574–577 (2012).
3. R. Kolesov, B. Grotz, G. Balasubramanian, R. J. Stöhr, A. A. L. Nicolet, P. R. Hemmer, F. Jelezko, and J. Wrachtrup, "Wave–particle duality of single surface plasmon polaritons," Nat. Phys. **5**(7), 470–474 (2009).
4. F. J. Rodríguez-Fortuño, G. Marino, P. Ginzburg, D. O'Connor, A. Martínez, G. A. Wurtz, and A. V. Zayats, "Near-field interference for the unidirectional excitation of electromagnetic guided modes," Science **340**(6130), 328–330 (2013).
5. D. Chang, A. Sørensen, P. Hemmer, and M. Lukin, "Strong coupling of single emitters to surface plasmons," Phys. Rev. B **76**(3), 035420 (2007).
6. P. Biagioni, J. S. Huang, and B. Hecht, "Nanoantennas for visible and infrared radiation," Rep. Prog. Phys. **75**(2), 024402 (2012).
7. V. Giannini, A. I. Fernández-Domínguez, S. C. Heck, and S. A. Maier, "Plasmonic nanoantennas: fundamentals and their use in controlling the radiative properties of nanoemitters," Chem. Rev. **111**(6), 3888–3912 (2011).
8. G. Grzela, R. Paniagua-Domínguez, T. Barten, Y. Fontana, J. A. Sánchez-Gil, and J. Gómez Rivas, "Nanowire antenna emission," Nano Lett. **12**(11), 5481–5486 (2012).
9. A. Ono, J.-I. Kato, and S. Kawata, "Subwavelength Optical Imaging through a Metallic Nanorod Array," Phys. Rev. Lett. **95**(26), 267407 (2005).
10. C. Höppener and L. Novotny, "Exploiting the light-metal interaction for biomolecular sensing and imaging," Q. Rev. Biophys. **45**(02), 209–255 (2012).
11. N. J. Halas, S. Lal, W. S. Chang, S. Link, and P. Nordlander, "Plasmons in strongly coupled metallic nanostructures," Chem. Rev. **111**(6), 3913–3961 (2011).
12. H. Wei, Z. Li, X. Tian, Z. Wang, F. Cong, N. Liu, S. Zhang, P. Nordlander, N. J. Halas, and H. Xu, "Quantum dot-based local field imaging reveals plasmon-based interferometric logic in silver nanowire networks," Nano Lett. **11**(2), 471–475 (2011).
13. H. Wei and H. Xu, "Nanowire-based plasmonic waveguides and devices for integrated nanophotonic circuits," Nanophotonics **1**(2), 155–169 (2012).

#209128 - $15.00 USD Received 31 Mar 2014; revised 6 Jun 2014; accepted 8 Jun 2014; published 18 Jun 2014

14. S. Kumar, A. Huck, Y. Chen, and U. L. Andersen, "Coupling of a single quantum emitter to end-to-end aligned silver nanowires," Appl. Phys. Lett. **102**(10), 103106 (2013).
15. D. E. Chang, A. S. Sørensen, E. A. Demler, and M. D. Lukin, "A single-photon transistor using nanoscale surface plasmons," Nat. Phys. **3**(11), 807–812 (2007).
16. I. Aharonovich, A. D. Greentree, and S. Prawer, "Diamond photonics," Nat. Photonics **5**(7), 397–405 (2011).
17. J. E. Kennard, J. P. Hadden, L. Marseglia, I. Aharonovich, S. Castelletto, B. R. Patton, A. Politi, J. C. F. Matthews, A. G. Sinclair, B. C. Gibson, S. Prawer, J. G. Rarity, and J. L. O'Brien, "On-Chip Manipulation of Single Photons from a Diamond Defect," Phys. Rev. Lett. **111**(21), 213603 (2013).
18. V. N. Mochalin, O. Shenderova, D. Ho, and Y. Gogotsi, "The properties and applications of nanodiamonds," Nat. Nanotechnol. **7**(1), 11–23 (2011).
19. C. R. Martin, "Membrane-based synthesis of nanomaterials," Chem. Mater. **8**(8), 1739–1746 (1996).
20. G. E. Thompson, "Porous anodic alumina: Fabrication, characterization and applications," Thin Solid Films **297**(1-2), 192–201 (1997).
21. S. Shingubara, "Fabrication of nanomaterials using porous alumina templates," J. Nanopart. Res. **5**(1/2), 17–30 (2003).
22. Z.-K. Zhou, M. Li, Z.-J. Yang, X.-N. Peng, X.-R. Su, Z.-S. Zhang, J.-B. Li, N.-C. Kim, X.-F. Yu, L. Zhou, Z.-H. Hao, and Q.-Q. Wang, "Plasmon-Mediated Radiative Energy Transfer across a Silver Nanowire Array via Resonant Transmission and Subwavelength Imaging," ACS Nano **4**(9), 5003–5010 (2010).
23. O. Benson, "Assembly of hybrid photonic architectures from nanophotonic constituents," Nature **480**(7376), 193–199 (2011).
24. A. V. Akimov, A. Mukherjee, C. L. Yu, D. E. Chang, A. S. Zibrov, P. R. Hemmer, H. Park, and M. D. Lukin, "Generation of single optical plasmons in metallic nanowires coupled to quantum dots," Nature **450**(7168), 402–406 (2007).
25. A. Huck, S. Kumar, A. Shakoor, and U. L. Andersen, "Controlled Coupling of a Single Nitrogen-Vacancy Center to a Silver Nanowire," Phys. Rev. Lett. **106**(9), 096801 (2011).
26. A. González-Tudela, P. A. Huidobro, L. Martín-Moreno, C. Tejedor, and F. J. García-Vidal, "Theory of Strong Coupling between Quantum Emitters and Propagating Surface Plasmons," Phys. Rev. Lett. **110**(12), 126801 (2013).
27. W. Pfaff, A. Vos, and R. Hanson, "Top-down fabrication of plasmonic nanostructures for deterministic coupling to single quantum emitters," J. Appl. Phys. **113**(2), 024310 (2013).
28. J. Wolters, G. Kewes, A. W. Schell, N. Nüsse, M. Schoengen, B. Löchel, T. Hanke, R. Bratschitsch, A. Leitenstorfer, T. Aichele, and O. Benson, "Coupling of single nitrogen-vacancy defect centers in diamond nanocrystals to optical antennas and photonic crystal cavities," Phys. Status Solidi B **249**(5), 918–924 (2012).
29. J. Barthes, A. Bouhelier, A. Dereux, and G. Colas des Francs, "Coupling of a dipolar emitter into one-dimensional surface plasmon," Sci. Rep. **3**, 2734 (2013).
30. A. G. Curto, T. H. Taminiau, G. Volpe, M. P. Kreuzer, R. Quidant, and N. F. van Hulst, "Multipolar radiation of quantum emitters with nanowire optical antennas," Nat. Commun. **4**, 1750 (2013).
31. A. G. Curto, G. Volpe, T. H. Taminiau, M. P. Kreuzer, R. Quidant, and N. F. van Hulst, "Unidirectional emission of a quantum dot coupled to a nanoantenna," Science **329**(5994), 930–933 (2010).
32. T. Hümmer, F. J. García-Vidal, L. Martín-Moreno, and D. Zueco, "Weak and strong coupling regimes in plasmonic QED," Phys. Rev. B **87**(11), 115419 (2013).
33. I. D. Rukhlenko, D. Handapangoda, M. Premaratne, A. V. Fedorov, A. V. Baranov, and C. Jagadish, "Spontaneous emission of guided polaritons by quantum dot coupled to metallic nanowire: Beyond the dipole approximation," Opt. Express **17**(20), 17570–17581 (2009).
34. A. Mohammadi, V. Sandoghdar, and M. Agio, "Gold nanorods and nanospheroids for enhancing spontaneous emission," New J. Phys. **10**(10), 105015 (2008).
35. L. Rogobete, F. Kaminski, M. Agio, and V. Sandoghdar, "Design of plasmonic nanoantennae for enhancing spontaneous emission," Opt. Lett. **32**(12), 1623–1625 (2007).
36. P. B. Johnson and R. W. Christy, "Optical Constants of the Noble Metals," Phys. Rev. B **6**(12), 4370–4379 (1972).
37. J. Takahara, S. Yamagishi, H. Taki, A. Morimoto, and T. Kobayashi, "Guiding of a one-dimensional optical beam with nanometer diameter," Opt. Lett. **22**(7), 475–477 (1997).
38. J. Zuloaga, E. Prodan, and P. Nordlander, "Quantum Plasmonics: Optical Properties and Tunability of Metallic Nanorods," ACS Nano **4**(9), 5269–5276 (2010).
39. D. E. Chang, A. S. Sørensen, P. R. Hemmer, and M. D. Lukin, "Quantum Optics with Surface Plasmons," Phys. Rev. Lett. **97**(5), 053002 (2006).
40. M. S. Tame, K. R. McEnery, Ş. K. Özdemir, J. Lee, S. A. Maier, and M. S. Kim, "Quantum plasmonics," Nat. Phys. **9**(6), 329–340 (2013).
41. D. E. Gómez, A. Roberts, T. J. Davis, and K. C. Vernon, "Surface plasmon hybridization and exciton coupling," Phys. Rev. B **86**(3), 035411 (2012).
42. G. Toscano, S. Raza, W. Yan, C. Jeppesen, S. Xiao, M. Wubs, A.-P. Jauho, S. I. Bozhevolnyi, and N. A. Mortensen, "Nonlocal response in plasmonic waveguiding with extreme light confinement," Nanophotonics **2**(3), 161–166 (2013).
43. E. Cubukcu and F. Capasso, "Optical nanorod antennas as dispersive one-dimensional Fabry–Pérot resonators for surface plasmons," Appl. Phys. Lett. **95**(20), 201101 (2009).

#209128 - $15.00 USD Received 31 Mar 2014; revised 6 Jun 2014; accepted 8 Jun 2014; published 18 Jun 2014

44. H. Ditlbacher, A. Hohenau, D. Wagner, U. Kreibig, M. Rogers, F. Hofer, F. R. Aussenegg, and J. R. Krenn, "Silver Nanowires as Surface Plasmon Resonators," Phys. Rev. Lett. **95**(25), 257403 (2005).
45. W. L. Barnes, "Surface plasmon–polariton length scales: a route to sub-wavelength optics," J. Opt. A, Pure Appl. Opt. **8**(4), S87–S93 (2006).
46. L. Novotny, "Effective Wavelength Scaling for Optical Antennas," Phys. Rev. Lett. **98**(26), 266802 (2007).
47. J. Takahara and M. Miyata, "Mutual mode control of short- and long-range surface plasmons," Opt. Express **21**(22), 27402–27410 (2013).
48. S. Zhang, H. Wei, K. Bao, U. Håkanson, N. J. Halas, P. Nordlander, and H. Xu, "Chiral Surface Plasmon Polaritons on Metallic Nanowires," Phys. Rev. Lett. **107**(9), 096801 (2011).

1. Introduction

Understanding the coupling between a quantum emitter and a waveguide is scientifically and technologically extremely valuable because it provides a flexible bridge between optics and electronics. From a scientific point of view, it permits testing some of the most fundamental aspects of physics, such as quantum entanglement [1], plasmon tunneling [2], wave-particle duality [3], near-field interference [4] and the strong coupling of light to emitter systems [5]. Careful evaluation and control of this coupling will allow for development of efficient hybrid photonic/plasmonic devices with the maximum coupling between an optical emitter and a plasmonic waveguide. Targeted and efficient energy transfer is also important in other related coupled systems and devices, such as nanoantenna [6–8], nanolenses [9], biosensors [10] and in coupled metallic devices [11]. These applications have progressed breakthroughs in technology for variety of applications, including switching [12, 13], photon splitter [14], single photon transistor [15] and microscopy [6].

Two key elements of coupled optical-plasmonic systems are emitters and waveguides. Quantum dots and impurities and defects in crystal structures are promising candidates for quantum emitters. Nitrogen vacancy (NV) centers in nanodiamonds are one of the most attractive single photon emitters available because they are stable, coherent and have strong emission at room temperature [16, 17]. NV centers have emission in the visible and near infrared range, which makes them also suitable for a range of biomedical applications [18]. Metallic nanostructures are used as a waveguide, because they can enhance the emission characteristic of a nearby emitter via near-field interactions [11]. One of the main drawbacks of metal structures is Ohmic losses at optical frequencies, which leads to loss of photons before they reach the target. Hence low loss metals such as silver, aluminum and gold are often employed for this purpose. The advantage of silver is that it has got plasmon resonances in the visible range of the spectrum. Metallic nanowires can be fabricated by a variety of synthesis methods. The template growth of the metallic nanowires has been extensively investigated because it offers unique control over nanowire diameter and length [19]. The most commonly used template is anodic aluminum oxide (AAO), which can be easily synthesized using electro chemistry methods [20]. AAO provides a unique template platform for fabrication of 1D nanostructures such as nanowires [21] because it has tunable and uniform pore sizes ranging from 10 nm to 450 nm, controllable shape and interpore distances. Metallic nanowires (NWs) fabricated with this method have been demonstrated experimentally to guide light via the excitation of surface plasmons [22].

In the last few years, there have been several experimental and theoretical studies into the coupling between photon emitters and metallic nanostructures [1, 5, 7, 14, 23–33]. For example, Akimov *et al.* [24] have experimentally studied coupling of a single photon emitter to the surface plasmons in a silver nanowire. In their study it was observed that the coupling is stronger for a nanowire with 100 nm diameter compared to the 50 nm diameter nanowire. Chang *et al*. [5] have proposed tapered shaped nanowires for improved coupling between a quantum emitter and a nanowire to achieve a strong coupling. It was reported that quantum dots deposited on one end of an array of vertical silver nanowires can excite surface plasmons along the nanowires, and the propagated plasmons can excite quantum dots at the other end of the NWs [22]. Different geometries and designs have been proposed for enhancing spontaneous emission of a single emitter coupled to gold nanostructures [34, 35]. However,

#209128 - $15.00 USD Received 31 Mar 2014; revised 6 Jun 2014; accepted 8 Jun 2014; published 18 Jun 2014

despite significant progress in this field in the recent years, a detailed understanding of different factors influencing the transmitted power characteristics and coupling between an optical emitter and a nanowire plasmonic waveguide has not been undertaken to date. Good theoretical knowledge of the effective parameters will be important for designing efficient emitter-waveguide devices.

Here, we report on a rigorous computational study of the coupling between a quantum emitter and a finite-size vertical silver nanowire embedded in an alumina matrix using a finite elements method. We present a comprehensive description of the effective parameters in a realistic coupled emitter-nanowire system and optimize the system for optimal coupling between the quantum emitter and plasmons in the silver nanowire. This study takes into account several realistic considerations, such as finite length of the nanowires, lossy nature of materials and retardation effects. We study the effects of the nanowire length, nanowire diameter, distance between the dipole and the nanowire, orientation of the emitter and refractive index of the surrounding media. We show how a combination of these parameters can be used to obtain the strongest transmitted power with Purcell factor of the order of 100. The detailed knowledge of the effective parameters can be applied in different applications, such as sensing, communication and lensing, to achieve more efficient coupling in these devices.

This paper is organized as follows. In section 2, we summarize the physical basis and simulation methods. In section 3, the effect of different parameters on coupling is investigated and described. In section 4, we present the optimum conditions for obtaining the maximum coupling using a specific emitter wavelength.

Some terms are used interchangeably with regarding the suitability of the context: *waveguide* for the nanowire and also *dipole* and *emitter* for the NV center in nanodiamond.

2. Physical basis and methods

The geometry of the system used in the calculations of the coupling between a quantum emitter and a vertical finite-size nanowire is shown schematically in Fig. 1. A single silver nanowire with length L and diameter D is embedded in a nanopore of a homogeneous dielectric template with refractive index n_d. In this work, the template is considered to be porous anodic aluminum oxide (AAO). A dipole emitter is placed on top of the nanowire along the long axis of the nanowire with a distance d from the top of the nanowire. The dipole emitter emits a light with a wavelength λ_0 (650 nm) and is oriented at an angle θ in respect to the long axis of the nanowire. We consider the dipole embedded in a spherical nanodiamond particle. The refractive index of the metallic nanowire is extracted and interpolated from Johnson and Christy [36]. The rest of the geometry is considered as vacuum ($n = 1$).

We use a finite element method (FEM) to solve Maxwell's equation for a coupled emitter-nanowire system using COMSOL Multiphysics (version 4.3b with RF module). The FEM is a powerful method to simulate electromagnetic field near or inside nanostructures. It can be applied to almost any geometry, with consideration of material dispersion via their permittivity and permeability. For our simulation purposes, the NV center in nanodiamond is modeled using a point electric dipole embedded at the center of a spherical domain, with a diameter of 20 nm and refractive index of 2.4. The dipole moment lies on xy plane and the oscillation wavelength is set to be 650 nm. Since it is challenging to accurately determine the dipole orientation or position in an experimental setup, we study the effect of both of these parameters in our calculations. The calculation region consists of a 3D spherical domain with 3.2 μm diameter with scattering boundary conditions to minimize reflections from the boundaries of the system. Adaptive mesh refinement is used to discretize the geometry using a triangular mesh with a minimum and maximum grid size of 1/20 and 1/10 of the nanowire diameter.

#209128 - $15.00 USD Received 31 Mar 2014; revised 6 Jun 2014; accepted 8 Jun 2014; published 18 Jun 2014

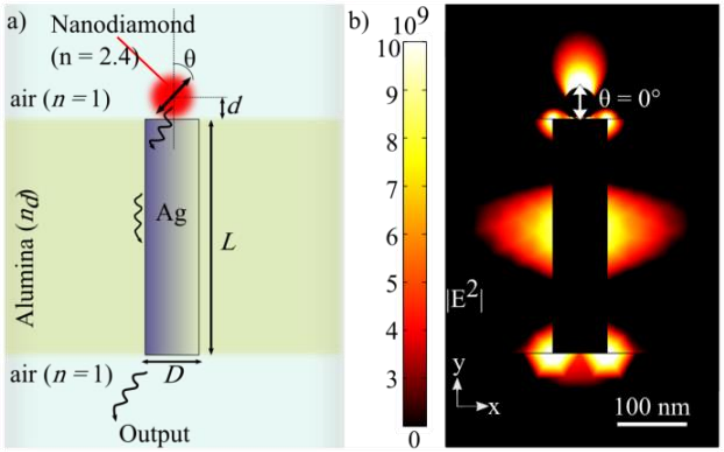

Fig. 1. a) Schematics of the 2D cross-section of the coupled nanowire-nanodiamond system. b) 2D intensity plot of the calculated electric field of propagating surface plasmons in a silver nanowire coupled to a dipole emitter with an emission wavelength of 650 nm. The emitter is represented by a single NV center in nanodiamond, which is placed on top of the nanowire with a 10 nm spacing from its surface. The dipole emitter is oscillating in *y* axis. The silver nanowire is 240 nm long, 70 nm in diameter and is embedded in alumina.

We define the "transmitted power" and "reflected power" as the time-averaged power emitting from the bottom and top ends of the nanowire, respectively. A spherical domain with 1.6 μm diameter is used to integrate over the time-averaged power in space. Upper hemisphere and lower hemisphere correspond to transmitted and reflected power respectively. The reference power (P_0) is taken from a system with exactly same geometry and frequency, with all the space and materials to be vacuum (n = 1) except the nanodiamond region (n = 2.4). All the results are normalized to the corresponding reference value.

The modes supported by the nanowire are obtained by solving the full three-vector Maxwell's equations for a lossy medium in the frequency domain. By applying the proper boundary conditions in Maxwell's equations, for a waveguide (nanowire) embedded in a dielectric, one can resolve the characteristic equation of the 0th-order transverse magnetic mode (TM_0) [37]. The solutions are complex propagation constants of the propagated waves inside the nanowire, which are a function of radius of the nanowire (R), dielectric properties and frequency [37].

The mechanism of the coupling has been the subject of many previous studies which belong within the context of "quantum plasmonics" [24, 26, 38–41]. Briefly, the existence of a metallic nanostructure in the near-field of a quantum emitter increases the local density of the states (LDOS), providing more quantum states for the excited atom to relax (Fermi's golden rule). This will affect the decay behavior of the quantum emitter, in terms of emission rates and probability of emission to different channels (radiative and non-radiative). The maximum of the density of states is within the plasmon resonance wavelength, which makes it more probable for an excited atom to decay into the plasmonic channel (coupling) [5]. Despite its quantum nature, the behavior of a coupled system can be observed at the macroscopic scales [24]. So by careful considerations of dimensions, one should be able to study the effective parameters of coupling in the classical regime (Maxwell's equations) [38]. We also tried to avoid quantum mechanical effects (such as tunneling and non-local effects) by considering the minimum diameter of 10 nm and minimum distance between the emitter and the nanowire of 10 nm. At distances below 10 nm quantum effects become more important and because of classical nature of our FEM calculations, we cannot get reliable results at those small distances [38, 40, 42].

#209128 - $15.00 USD Received 31 Mar 2014; revised 6 Jun 2014; accepted 8 Jun 2014; published 18 Jun 2014

3. Results and discussion

3.1 Effect of nanowire length

The amount of transmission demonstrates a strong dependence on the length of the nanowires. Figure 2 shows the effect of nanowire length on the transmitted power of the system for a nanowire (D = 70 nm) at emission wavelengths (λ_0) of 650 nm. The transmitted power is not only dependent on nanowire length but also varies as a function of nanowire diameter (D) and wavelength (λ). Despite this, we can extract the overall nanowire length dependence of the transmitted power when using a constant D and λ values. Generally, the nanowire length-transmitted power behavior exhibits two main distinct features: (i) sinusoidal oscillations and (ii) a decay of the power with an increasing nanowire length. Each of these behaviors originates from different mechanisms as described below.

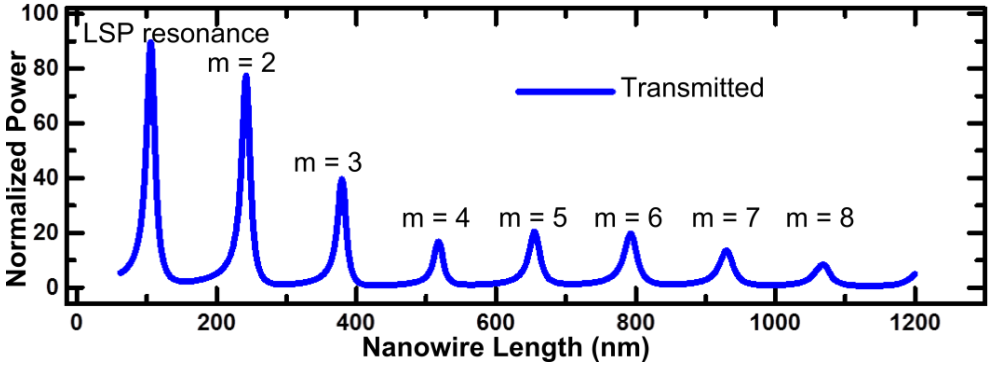

Fig. 2. Transmitted power vs. nanowire length for nanowires of D = 70 nm embedded in alumina (n_d = 1.6). The emission wavelength is at λ_0 = 650 nm. The emitter is set 10 nm above the nanowire and is oscillating in the y direction.

(i) Sinusoidal oscillations- At resonant lengths, the transmitted power has its relative maximum value. It is phenomenologically equal to a plasmonic Fabry-Perot (FP) cavity [43, 44], where the ends of the wire naturally act as mirrors facing each other and partly reflecting back the plasmons. The resonance length of nanowire versus the order of the resonance is a constant number (L_{res}/m = const.), which is one of the characteristics of FP resonance. The formed standing waves possess maxima and minima that correspond to constructive and destructive interference between forward and backward propagating plasmons, respectively. The conditions for the resonance in a FP cavity are [43]:

$$L(\lambda, D) = \frac{m\lambda(D)}{2} + \Omega, \tag{1}$$

where m is an integer and λ is the wavelength of the wave in the cavity with length L and Ω is a constant which arises due to the phase changes and penetration of the field to free space at terminations of the cavity.

Short nanowires (e.g. L <~100 nm) behave more as nanoparticles and therefore localized surface plasmons start to play a dominant role. Additionally, the whole nanoparticle (short nanowire) can act as a dipole due to an external electric field that can cause a separation of charge, giving rise to a maximum peak in the emission spectrum [41]. This dipole effect can mean that there is no formation of surface plasmon polaritons (SPPs), and consequently of no FP effect in these short wires. Since in our case, for m = 1, λ is in the range of ~240 nm, it is expected that the first FP resonance will be at ~λ/2 which corresponds to the nanowires of length ~120 nm. At this length scale localized surface plasmons (LSPs) are formed and as a consequence there is no FP resonance at m = 1, and FP resonances appear only for higher modes (m = 2, 3 …). The strongest FP peak is at m = 2, due to the minimum losses (as

#209128 - $15.00 USD Received 31 Mar 2014; revised 6 Jun 2014; accepted 8 Jun 2014; published 18 Jun 2014

described below). It is also worthwhile mentioning that generally thinner (D = 50 nm) nanowires exhibit sharper and stronger spectral peaks at different wavelengths compared to thicker wires (D = 100 nm). This corresponds to a higher quality of the FP cavity, due to the higher reflection. The higher reflection arises from a shorter wavelength and a higher momentum mismatch at the interface.

(ii) Decay behavior - The transmitted power generally decays as $e^{-k''L}$, where k'' is the imaginary part of the SPP wave vector ($k = k' + ik''$) and L is the length of the nanowire [45]. k'' represents Ohmic losses along the metal structure. As a result it is expected that there will be higher losses in longer nanowires. Propagation length (L_{spp}) of the surface plasmons is also inversely related to k''. Generally, the lower the value of k'', the lower the loss and the longer the propagation length.

3.2 Effect of nanowire diameter

Our results show that the diameter of the silver nanowires plays an important role in the dipole-plasmon coupling. Figure 3 shows the influence of nanowire diameter on the transmitted power of the coupled system at the emission wavelength of λ_0 = 650 nm. Two different behaviors are seen in Fig. 3. For small diameters (D), the output increases as a function of diameter up to 70 nm. In this regime, sharp peaks are formed at certain diameters when the total energy reaches a local maximum value. For thicker nanowires with diameter > 70 nm, the behavior of the transmitted power shows an exponential decrease with increasing diameter.

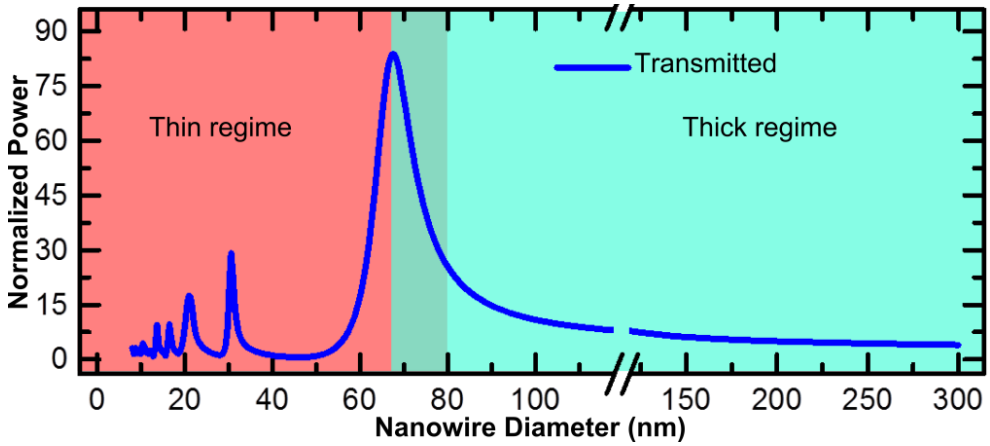

Fig. 3. Transmitted power vs. nanowire diameter in "thin" (left) and "thick" (right) regimes. (L = 240 nm).

(i) Thin nanowires- In this regime, the transmitted power is very sensitive to the diameter of the nanowire. Figure 3 (left) shows the transmitted and reflected power of a 240 nm long silver nanowire in a thin nanowire regime. It can be seen that the transmitted power and reflected power oscillate and increase with increasing diameter. Transmission of electromagnetic waves happens inside a metallic nanowire at the thicknesses around the skin depth. This transmission is strongly influenced by the nanowire thickness. As a result of this phenomenon, an incident electromagnetic wave on a thin metal nanowire can affect the charge distribution of the whole nanowire including surface and volume charges. If the metal is considered as a lossless material, these charge oscillations are equivalent to plasma oscillations (ω_p). These plasma oscillations can propagate along a metal nanowire with their fundamental mode (TM_0). There is no cut-off for this axially symmetric mode and this mode exists even when the diameter approaches zero. This mode is a result of oscillations of electrons parallel to the axis (longitudinal) of nanowire. The propagation constant is a

#209128 - $15.00 USD Received 31 Mar 2014; revised 6 Jun 2014; accepted 8 Jun 2014; published 18 Jun 2014

function of diameter and both real and imaginary parts of the *k* vector are bigger for thinner nanowires. The higher imaginary part of *k* means more confinement of the electromagnetic wave and higher Ohmic losses. The higher real part causes a bigger momentum mismatch at the end of the nanowire and less transmission. Therefore we expect an increase in the transmitted power for thicker nanowires at this regime. The simulated results match the expected trend, with the exception of the resonance points.

At resonance conditions, the charge distribution has its relative maximum at the ends of nanowires. The expected resonance thickness (diameter) of a given-length of nanowire can be predicted according to Novotny, using antenna theory [46]. According to this picture, a nanowire behaves like an antenna at optical frequencies. At the resonance of the antenna, the nanowire is polarized and the effective resonance wavelength ($\lambda_{eff\text{-}res}$) of the system can be estimated as [46]:

$$\frac{\lambda_{eff-res}}{2\pi R} = 13.74 - 0.12[\varepsilon_\infty - \varepsilon_s 141.04]/\varepsilon_s - \frac{2\pi}{N} + \frac{\lambda}{\lambda_p} 0.12\sqrt{\varepsilon_\infty + \varepsilon_s 141.04}/\varepsilon_s, \qquad (2)$$

where $\lambda_{eff\text{-}res}$ is the effective wavelength (scaled wavelength), λ_p and ε_∞ are the plasma resonance ($2\pi c/\omega_p$) and permittivity of bulk silver, respectively. ε_s is the permittivity of alumina and *N* is the mode of the resonance. Additionally, we expect the resonant wavelength for a given length of the nanowire to satisfy this condition:

$$L_{res} = \frac{N\lambda_{eff-res}}{2}. \qquad (3)$$

Other parameters, such as out-of-resonance lengths, different angle of emission and formation of the different modes (in addition to TM_0), start also affecting the resonance modes [44, 47], which are only considered in the FEM approach but not in the analytical approach.

(ii) Thick nanowires- As the nanowires become thick enough, photon tunneling reduces in the material and there will be an exponential decay of transmitted power by increasing the diameter (*D*) of nanowire. This decay behavior mainly originates from the higher reflection from the top surface of the thicker nanowires.

As the thickness of the nanowire increases, the higher modes of propagation form along the nanowire. In addition of the fundamental TM_0 mode, there are two other modes in nanowires which correspond to the transverse oscillations of the electrons (HE_1 and HE_{-1}) [5, 47]. Consequently the Eq. (2) is not adequate to calculate the effective wavelength.

To gain a more physical insight into the influence of the nanowire diameter we have plotted the normalized electric field along a silver nanowire for different diameters in Fig. 4. By counting the number of the maxima in Fig. 4 one can easily realize that the wave vector (or wavelength) of the surface plasmons is changed as a function of the nanowire diameter. Thinner nanowires (10, 30, 50 nm) have bigger k_{spp} (shorter λ_{spp}) compared to thicker nanowires (70, 100, 300 nm). The number of the peaks (wave vector) remains almost constant when $D > 70$ nm.

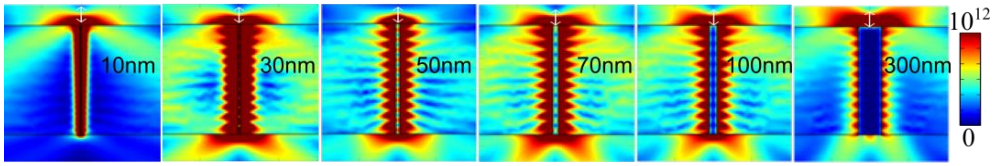

Fig. 4. (2D model) Normalized electric field along a silver nanowire with different diameters, $L = 2$ μm, and $\lambda_0 = 650$ nm. The clear change of the wave vector (by counting the number of maxima) is observed by changing the diameter.

#209128 - $15.00 USD Received 31 Mar 2014; revised 6 Jun 2014; accepted 8 Jun 2014; published 18 Jun 2014

3.3 Effect of NV center position relative to the nanowire

The dipole emitter can have different positions relative to the nanowire. Its position can vary vertically and horizontally from the center position. The role of vertical and horizontal distance of the NV center is shown in Fig. 5.

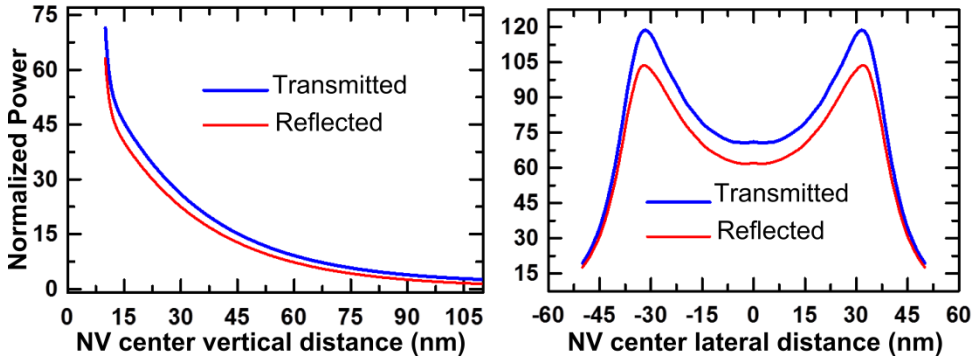

Fig. 5. (left) Transmitted power and reflected power vs. dipole vertical distance from the top surface of the nanowire, (d_x = 0 nm), (right) Transmitted power and reflected power vs. dipole horizontal distance from the nanowire (d_y = 10 nm). (D = 70 nm, L = 240 nm).

(i) Vertical distance – Here we study the influence of the vertical distance of the nanodiamond with respect to the nanowire on the transmitted and reflected power, while the diameter of the nanodiamond is considered to be constant (20 nm). Figure 5(left) shows that the power decreases approximately exponentially with the vertical distance of the nanodiamond. The transmitted power of the system is expected to drop by increasing the distance between the emitter and nanowire. However, both the propagation mode and the propagation constant are not influenced significantly by the vertical position of the dipole. The decay of the power can be partly attributed to the contribution of both decaying fields of the nanowire and dipole. The exact dependency is slightly more complicated because the emission rates of an emitter depend on the electric field and also local density of states in its vicinity [5]. The non-radiative decay rate is also increasing with the distance between the nanowire and the dipole [5].

(ii) Horizontal distance – The effects of the dipole horizontal position (in the center of nanodiamond) relative to the nanowire are shown in Fig. 5(right). It is clear that as the dipole moves from the center to edges, the power increases and as the dipole crosses the edge of the nanowire, there is a rapid drop down of the transmitted power. This behavior is expected since the electric field is expected to get stronger around the edges of the nanowire. The stronger field will provide more LDOS channels for the emitted light to decay into, and as a result coupling is stronger and therefore higher transmitted power is expected.

In the simulations shown in above, the diameter of the nanodiamond is held fixed at 20 nm. However, we would expect the strength of coupling to depend on both the size of the nanodiamond and the position of the NV center within the diamond. Detail examination is outside the scope of this paper.

3.4 Effect of polarization of the emitter

Although in practice it is very hard to control polarization of a NV center in nanodiamond, it has a very significant effect on the strength of the coupling. Figure 6 shows the effect of the emission angle on transmitted power of the system. The maximum of the coupling is found for 0° (parallel to the nanowire axis) emission. There is a non-zero coupling at 90°, which arises from the near-field effects at the nanowire terminations. Figure 7 shows the intensity of electric field intensity (E^2) for a few different dipole orientations. The symmetry of the system

#209128 - $15.00 USD Received 31 Mar 2014; revised 6 Jun 2014; accepted 8 Jun 2014; published 18 Jun 2014

is broken at $0° < \theta < 90°$. This gives rise to HE_1 and HE_{-1} modes to contribute jointly with TM_0 mode by forming a new superimposed mode [48].

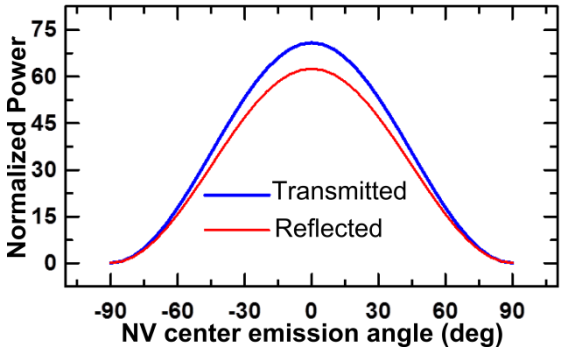

Fig. 6. Transmitted power and reflected power vs. dipole orientation (D = 70 nm, L = 240 nm).

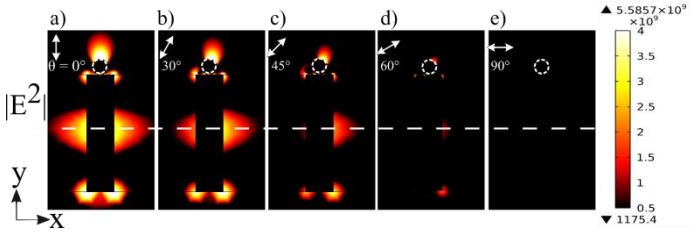

Fig. 7. Electric field along a silver nanowire near a dipole with different orientations: 0, 30, 45, 60 and 90° (D = 70 nm, L = 240 nm).

3.5 Effect of refractive index of the environment

The refractive index of the surrounding environment can strongly affect the wavelength of the propagating plasmons and so change the transmitted power (Fig. 8). The propagation constant is shorter for low refractive index materials than high refractive index materials. Figure 9 shows the effect of dielectric refractive index of the surrounding material around the nanowire on transmitted power for three different nanowire lengths. We observe several maxima and oscillations in the spectra which are due to the finite size of the nanowire and reflections from the nanowire ends. The origin of these sharp peaks is again due to the FP resonances. It is clear that for a longer nanowire there will be more oscillations as a result of more allowed resonance modes. We have found that the oscillations in shorter nanowires are more sensitive to refractive index of the surrounding dielectric, giving rise to stronger resonances.

The maximum power of a 240 nm long nanowire is at n_d = 1.6, because we have optimized the other parameters with this value. The narrow peaks in Fig. 9 show that this system is very sensitive to small changes of refractive index.

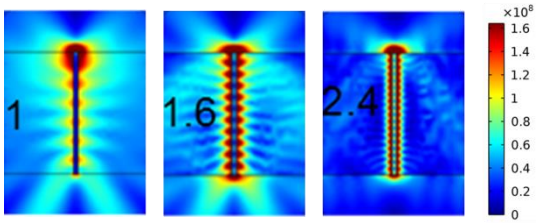

Fig. 8. (2D model).Normalized electric field along a silver NW surrounded by a material with different refractive index (1, 1.6, 2.4). (D = 70 nm, L = 2 μm).

#209128 - $15.00 USD Received 31 Mar 2014; revised 6 Jun 2014; accepted 8 Jun 2014; published 18 Jun 2014

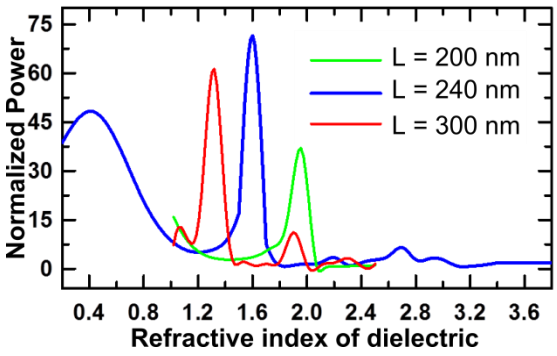

Fig. 9. Transmitted power as a function of refractive index of the surrounding material for three different nanowire lengths (L = 200, 240 and 300 nm, D = 70 nm).

4. Purcell factor

In the previous section we have studied different effective parameters of the coupled system consisting of an emitter and a finite-size lossy metal nanowire. It has been shown that most of the parameters are not independent of each other and therefore it is a very complicated task to find a general formulization for this system. However, a proper understanding of each effect can assist in finding an approach for optimizing the system for a maximum coupling. In the literature the measure of the strength of coupling is usually expressed by Purcell factor. To calculate the Purcell factor, the transmitted power of the emitter is calculated in the presence and absence of other dielectrics (P/P_0). Therefore all the normalized data that we have presented in this work are equivalent to the Purcell factor.

Figure 10 shows the surface charge distribution, far-field and the value of Purcell factor for the three strongest coupling configurations. Our results show that high Purcell factor, as high as 119, is achievable in this system. The optimization has been done by using realistic parameters in our model for a silver nanowire, n_d = 1.6 for alumina and λ_0 = 650 nm for NV center in nanodiamond. The optimum length of the nanowire was found at L_{max} = 240 nm, which is equal to the position of the first FP resonance (m = 2). Although higher Purcell factor is calculated for L = 90 nm in Fig. 10(left), this system does not represent a nanowire anymore but rather a nanoparticle. In this case, there is no FP resonance (m = 1), as mentioned in section 3.1, and the observed resonance is originating from the formation of local surface plasmons. The optimum diameter of the nanowire, D_{max} = 68 nm, is obtained at the border line of "thin" and "thick" regime. We have found that Purcell factor very strongly depends on nanowire diameter and even a very small change of the diameter from the optimum leads to a drastic decrease of Purcell factor. For example when D = 68 ± 3 nm, the Purcell factor drops by 10%. The optimum vertical distance of the dipole and nanowire is found at 10 nm (without consideration of smaller distances due to the quantum effects). The optimum emission angle (θ) is 0°. The highest Purcell factor is achieved when the dipole is placed at the edge of the nanowire but this is at the cost of asymmetric emission from the nanowire, as shown in Fig. 10(right).

#209128 - $15.00 USD Received 31 Mar 2014; revised 6 Jun 2014; accepted 8 Jun 2014; published 18 Jun 2014

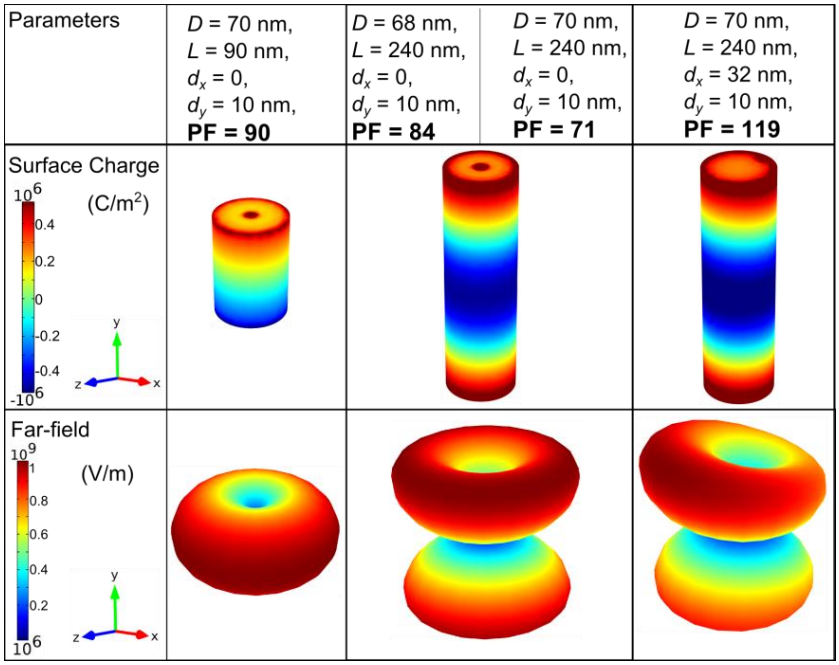

Fig. 10. Purcell factor (PF), surface charge and far-field for some of the modeled configurations. The dipole emitter in nanodiamond with an emission wavelength of 650 nm is oscillating in *y* axis. The silver nanowire is embedded in alumina (n_d = 1.6).

5. Conclusions

We have used finite elements method to study the coupling between an optical emitter and a nanowire in an alumina matrix. We have taken in to account realistic considerations such as finite size of the nanowire and losses in the nanowire. In this work we have studied the effects of the nanowire length, diameter and material, dipole position, polarization and the refractive index of the surrounding dielectric. The coupling strength has been judged by the measured normalized time-average power from the end of the nanowire. The observed contribution of each parameter has been studied individually and compared to other theoretical and experimental studies. We have demonstrated that the length of the nanowire can be adjusted to undergo Fabry-Perot resonances. The coupling has been found very sensitive to the diameter of the nanowire, and the effect of diameter was described within two regimes of thin- and thick nanowires. For the thin nanowires the volume charges inside of the nanowire are responsible for waveguiding. The situation is different for thick nanowires, where surface plasmon polaritons (SPPs) are the guiding tools. The highest coupling enhancement in a realistic single nanowire-emitter system consisting of a silver nanowire embedded in alumina and coupled to a nanodiamond emitter has been estimated and a Purcell factor of ~100 has been achieved. The presented results provide clear guidelines for fabrication of efficient coupled emitter-nanowire devices such as nanoantenna, biosensor, SERS, optical switch and plasmonic lenses.

Acknowledgments

The authors wish to acknowledge computational resources and facilities of the Australia's National Computational Infrastructure (NCI). We acknowledge financial support from the University of Melbourne research and CSIRO top-up scholarships.

#209128 - $15.00 USD Received 31 Mar 2014; revised 6 Jun 2014; accepted 8 Jun 2014; published 18 Jun 2014